



## Kinetics Studies of Palm Kernel Oil Ethanolysis Using Nigerian Clay as Catalyst Support

<sup>1</sup>Adekunle I. A., <sup>2</sup>Salam K. K., <sup>3</sup>Salawudeen T. O., <sup>4</sup>Arinkoola A. O.  
and <sup>5</sup>Dada E. O.

<sup>1</sup>National Board for Technology Incubation (NBTI-TIC, Ilorin), Federal Ministry of Innovation, Science and Technology, Abuja.

<sup>2,3,4,5</sup>Department of Chemical Engineering, Faculty of Engineering and Technology, Ladoke Akintola University of Technology, Ogbomoso, Nigeria.

<https://www.laujet.com/>



### Keywords:

Itu clay, Sulphuric acid,  
Kinetics. analysis

### Corresponding Author:

[kksalam@lautech.edu.ng](mailto:kksalam@lautech.edu.ng)

### ABSTRACT

*The kinetics study of palm kernel oil (PKO) ethanolysis using Itu/H<sub>2</sub>SO<sub>4</sub> catalyst was investigated to optimize biodiesel production. The study explored the reaction rate, activation energy and the influence of catalyst loading. The pseudo-first and pseudo-second-order kinetic models were applied to describe the reaction mechanism, revealing a significant dependency on temperature with activation energy values of 13,343.9 kJ/mol and 46,259.1 kJ/mol obtained for the pseudo-first and pseudo-second order models. The results demonstrated that the Itu/H<sub>2</sub>SO<sub>4</sub> catalyst effectively enhanced the ethanolysis process, achieving 96% biodiesel yield within a 2 h reaction time. The kinetics mechanism of the Itu/H<sub>2</sub>SO<sub>4</sub> catalyst is more favourable with a pseudo-second order reaction.*

### INTRODUCTION

The production of renewable energy is crucial for the reduction of harmful materials that are emitted or discharged into the environment during excessive use of fossil fuels. Biodiesel derived from inexpensive plant-based oil, such as palm kernel oil (PKO), can be a suitable alternative for replacing the conventional fossil fuel (Usman et al., 2024). Biodiesel consists of long chains of carboxylic acids of alkyl esters that are produced from various raw materials, including waste cooking oil, animal fats, energy crops, yeast lipids, and microalgae via the processes of esterification and transesterification (Javed et al., 2022).

Unrefined feedstock like palm kernel oil (PKO) can serve as a cheaper raw material to replace expensive refined oil for biodiesel production (Faisal et al., 2021). Meanwhile, the unrefined PKO is characterized by large amounts of free fatty acid (FFA). This may contribute to soap formation when alkali catalyst is employed during transesterification (Wang et al., 2022). However, the use of acid-catalysed esterification reduces the FFA content in the oil and further converts them to fatty acid ethyl esters (FAEE) (Meher et al., 2006). The acid-catalysed esterification process is slower than transesterification as a result of the low miscibility of alcohol with PKO. This leads to the reduction of the overall mass transfer, thereby decreasing the rate of reaction (Li et al., 2022).

On catalyst classification, heterogeneous and homogeneous catalysts have both positive and negative effects on the biodiesel production process. Due to their fewer disposal problems, high resistance to saponification, easy separation from liquid product and catalyst reusability, the heterogeneous catalytic process is more desirable than its homogeneous counterparts (Gholipour et al., 2020). Meanwhile, it has been documented that rare earth metals are the most suitable heterogeneous catalysts in biodiesel production (Pinzi et al., 2011), unfortunately, they are expensive, and their preparation is quite complex. Therefore, to enhance sustainability, the use of low-cost solid

heterogeneous catalysts from waste and naturally occurring materials is suggested (Yusuff et al., 2018). These catalysts are being investigated to replace their conventional homogeneous and enzyme counterparts, and this research constitutes a part of the investigation. Furthermore, to the best of our knowledge, there is no reported literature on the kinetic studies for the transesterification of palm kernel oil over acid-modified Itu bentonitic clay. Thus, the technique involving the use of modified heterogeneous acid catalyst in converting palm kernel oil to biodiesel is adopted for this present study.

Transesterification process consists of three consecutive and reversible reactions; the triglycerides (TG) reaction with ethanol (A) and consequently diglycerides (DG) and monoglycerides (MG) reactions to produce ethyl ester (EE) and glycerol (G) that are reversible (Feyzi et al., 2017; Zeinalipour-Yazdi, 2018). Equations 1 – 3 show the mentioned reactions, while Equation 4 summarizes them:



For the overall reaction,



In the present study, the effect of catalyst dosage was investigated for the heterogeneous catalysis transesterification of palm kernel oil using IC/H<sub>2</sub>SO<sub>4</sub>. To discover the adequate kinetic model for experimental data, the pseudo–first-order and pseudo–second-order models were utilized. The rate constants and activation energy values were also researched.

## **MATERIALS AND METHODS**

### **Materials**

Palm kernel oil, ethanol (99.8% purity, Merck), Itu clay from Itu local government area of Akwa-Ibom State (Latitude: 5° 12' 4.72" N; Longitude: 7° 59' 1.43" E) and H<sub>2</sub>SO<sub>4</sub> (98% purity, Qingdao) were used for the study. The Itu clay/H<sub>2</sub>SO<sub>4</sub> catalyst was produced by acid activation. 5 g of Itu clay was activated using 6.0 M H<sub>2</sub>SO<sub>4</sub> concentration, 60 °C reaction temperature at a stirring rate of 400 rpm for 7.5 minutes. Subsequently, the catalyst was washed with distilled water and dried in an electric oven operated at 110 °C for 2 h (Onukwuli *et al.*, 2018). Brunauer-Emmett-Teller analysis was used to characterize the catalyst produced. This was done to ascertain and compare its surface area, pore volume and pore size distribution with that of the clay sample used. The fatty acid composition of the palm kernel oil was determined by gas chromatography as shown in Table 1.

### **Methods**

Fatty acid ethyl esters (FAEEs) were produced by transesterification of palm kernel oil with ethanol in the presence of Itu/H<sub>2</sub>SO<sub>4</sub> catalyst. Experiments were conducted to choose the best catalyst amount (between 1, 3, and 5 wt%) at a constant molar ratio (ethanol: oil) of 12:1, reaction temperature of 338.15 K, and stirring rate of 600 rpm. The yield of ethyl ester production was measured after the reaction times of 1, 2 and 3 h. The catalyst amount with the highest yield was considered the best one (Gholipour *et al.*, 2020). The kinetic study experiment was conducted with the best catalyst amount, ethanol to oil molar ratio of 12 to 1, a stirring rate of 600 rpm and reaction temperatures of 318.15, 328.15 and 338.15 K. The yield of ethyl ester production was measured after the reaction

times of 1, 2 and 3 h. In addition, Equation 4 was used to simplify the analysis of the kinetics studies since the whole transesterification results ultimately in the production of FAEE.

**Table 1: GC–MS Result of PKO**

S/N	Component name	Chemical formula	Retention time (min)	Area (%)
1	Octanoic acid	C <sub>8</sub> H <sub>16</sub> O <sub>2</sub>	11.67	0.60
2	Decanoic acid	C <sub>10</sub> H <sub>20</sub> O <sub>2</sub>	18.98	1.04
3	Dodecanoic acid	C <sub>12</sub> H <sub>24</sub> O <sub>2</sub>	22.75	38.56
4	Tetradecanoic acid	C <sub>14</sub> H <sub>28</sub> O <sub>2</sub>	25.57	6.02
5	n-Hexadecanoic acid	C <sub>16</sub> H <sub>32</sub> O <sub>2</sub>	29.42	9.82
6	Octadecanoic acid	C <sub>18</sub> H <sub>36</sub> O <sub>2</sub>	29.63	0.20
7	Oleic acid	C <sub>18</sub> H <sub>34</sub> O <sub>2</sub>	31.26	14.89

Hence, all intermediate reaction products (DG and MG) can be ignored and a simple mathematical model of Equation 4 expresses the whole conversion as one step is studied. The reaction mechanism of transesterification of PKO at the above-mentioned temperatures was analysed using the pseudo-first and second order kinetic models (Oniyah *et al.*, 2015).

#### **Pseudo–First Order Model**

The model proposed by Gholipour *et al.* (2020) was adopted. An excess ethanol to oil molar ratio was used, hence, the concentration of ethanol remains constant in the course of the reaction. Thus, the rate of reaction is determined by the concentration of triglycerides (TG) in the system. In the absence of both external and internal resistance to mass transfer, the intrinsic kinetics was determined using the pseudo-first-order reaction (Olutoye *et al.*, 2016). Considering equation 4 as the main reaction and the assumption made (i.e., use of excess ethanol), the pseudo-first-order kinetic model is as follows:

$$\frac{-dC_{TG}}{dt} = k_1 C_{TG} C_A \quad 5$$

$C_{TG}$  is the concentration of triglyceride;  $C_A$  concentration of ethanol

When excess ethanol is used,

$$K = k_1 C_A \quad 6$$

Therefore, equation 6 becomes equation 7

$$\frac{-dC_{TG}}{dt} = K C_{TG} \quad 7$$

$$\frac{-dC_{TG}}{C_{TG}} = K dt \quad 8$$

Integrating equation 8 gave equation 9

$$\ln \left[ \frac{TG_0}{TG} \right] = Kt \quad 9$$

Or

$$-\ln(1 - X_{TG}) = Kt \quad 10$$

Meanwhile, each mole of triglyceride (TG) can be transesterified to produce 3 mol of ethyl ester. Hence,

$$X_{TG} = 1 - \frac{TG}{TG_0} = 1 - \frac{TG_0 - \frac{EE}{3}}{TG_0} = \frac{EE}{3TG_0} \quad 11$$

Assuming the molecular weight of TG ( $W_{TG}$ ) is about three times that of EE. ( $W_{EE}$ ), The amount of  $X_{TG}$  could be considered as yield or the amount of ethyl ester ( $X_{EE}$ ) produced. This can be expressed by equation 12

$$X_{TG} = \frac{EE}{3TG_0} = \frac{m_{EE}/W_{EE}}{3m_{TG_0}/W_{TG}} \approx \frac{m_{EE}/W_{EE}}{3m_{TG_0}/3W_{EE}} \approx \frac{m_{EE}}{m_{TG_0}} = X_{EE} \quad 12$$

Hence, equation 10 can be written as equation 13

$$\ln(1 - X_{EE}) = -Kt \quad 13$$

The first order model can be analysed by plotting the values of  $\ln(1 - X_{EE})$  against time (t) to obtain the rate constant K, i.e. the slope of the graph.

### Pseudo-Second Order Model

Here, the kinetic equation was viewed as a second-order response to TG concentration. Expressing equation 7 as a second-order

$$\frac{-dC_{TG}}{dt} = kC_{TG}^2 \quad 14$$

Separating variables, there is

$$\frac{dC_{TG}}{C_{TG}^2} = -kdt \quad 15$$

Further simplification of Equation 15 gives Equation 16

$$\frac{1}{C_{EE}} = kt + \frac{1}{C_{EE0}} \quad 16$$

The reaction rate k and integration constants ( $\frac{1}{C_{EE0}}$ ) can be estimated from the slope and intercept of the graphical plot of  $\frac{1}{C_{EE}}$  versus time (t), respectively.

### Activation Energy of the Reaction

At higher reaction temperature, the energy and activity of the reactant molecules increase, thereby increasing the rate of reaction. To calculate the activation energy of the PKO biodiesel, the reaction rate constant ( $k$ ) and Arrhenius equation (Equation 17; Gholipour *et al.*, 2020) were utilized:

$$k = A * \exp\left(\frac{-E_a}{RT}\right) \quad 17$$

Where k is the rate constant, A, pre-exponential factor, E<sub>a</sub>, activation energy, R, gas constant and T, temperature.

## RESULTS AND DISCUSSION

### BET Analysis of Raw Itu Clay (RIC) and H<sub>2</sub>SO<sub>4</sub> activated clay (catalyst) (AIC)

The textural properties of the AIC catalyst play significant roles in the catalytic reaction. The surface area, pore volume and pore size were determined by BET models, respectively. Table 2 shows the results of the BET surface area, pore volume and pore size of RIC and AIC, respectively. The textural properties of the catalyst were improved as H<sub>2</sub>SO<sub>4</sub> was used to modify RIC that was initially beneficiated. The surface area, pore volume and pore size of RI were 122.20 m<sup>2</sup>/g, 0.074 cm<sup>3</sup>/g, and 21.38 Å, while AIC exhibited an increase in the surface area, pore volume, and pore size to 212.35 m<sup>2</sup>/g, 0.45 cm<sup>3</sup>/g and 28.55 Å, respectively. These results implied the transformation of RIC after acid modification and suggest that H<sub>2</sub>SO<sub>4</sub> exposes the catalyst pores, thereby increasing the surface area of the catalyst as well as improving its activity in PKOB production (Yusuff, 2019).

**Table 2: Textural Properties of RIC and AIC**

Sample	Textural properties		
	BET surface area (m <sup>2</sup> /g)	Pore volume (cm <sup>3</sup> /g)	Pore size (Å)
RIC	122.20	0.074	21.38
AIC	212.35	0.45	28.55

### Effect of Catalyst and Reaction Time on Biodiesel Yield

The effect of catalyst dosage on FAEs yield was investigated within the range of 1.0-5.0 w% (Table3) and biodiesel produced at 338.15 K with ethanol to oil ratio of 12:1. From the table, increasing the catalyst dosage from 1 wt% to 3 wt % for 1 and 3 h reaction time affects biodiesel yield positively (at 1h; 89.20% to 94.80% and 3h; 89.60% to 91.60%, while the yield decreases to 93.60% and 89.60% at 1 and 3 h, respectively, as the catalyst dosage increases to 5 wt%. This is in defiance of the result obtained at 2 h. Here, increasing the catalyst dosage from 1 to 3 wt% resulted in a gradual decrease in the biodiesel yield. Therefore, increasing the catalyst above 1 wt% could make the mixture of reactants viscous and create separation problems that decrease the yield and quality of biodiesel. This is similar to the work of Gholipour *et al.* (2020), where biodiesel was produced using K<sub>2</sub>CO<sub>3</sub>/Al<sub>2</sub>O<sub>3</sub> catalyst. The highest yield observed at 1 wt% catalyst dosage and 2 h reaction time was considered as a constant parameter for the kinetic study.

**Table 3: Effects of Catalyst and Reaction Time on the Biodiesel Yield**

S/N	Catalyst dosage (wt%)	Reaction time (h)		
		1.00	2.00	3.00
		Biodiesel yield (%)		
1	1.00	89.20	96.00	89.60
2	3.00	91.20	91.20	91.60
3	5.00	90.40	90.40	89.60

### **Kinetics of Palm Kernel Oil Biodiesel Reactions**

The kinetic study was done on the stage between 60 to 180 min that the rate of reaction was considerable, with an optimum catalyst concentration (1 wt%, Itu/H<sub>2</sub>SO<sub>4</sub>) at 318.15 to 338.15 K. Pseudo first and second order reaction kinetics was assumed for the transesterification reaction of palm kernel oil biodiesel (PKOB) from Equation 13 and 16 respectively. To establish the correctness of these assumptions and estimate the values of the reaction constants  $k$  at various temperatures, plots of  $\ln(1-X_{EE})$  versus time (min) and  $1/(1-X_{EE})$  versus time at temperatures 318.15, 328.15 and 338.15 K were made for the pseudo first and second order reaction, respectively. The plots generated using values presented in Tables 5 to 7 are presented in Figures 1 to 6, while values of correlation coefficients  $R^2$  and rate constants that were determined from the slope of the trend line are presented in Table 4. The values of correlation coefficients ( $R^2$ ) of the pseudo first and second order reaction at 318.15 K and 328.15 K were higher than those obtained at 338.15 K, with the  $R^2$  value recorded for second order kinetics at 318.15 K having the highest value of 0.983. This is similar to the results reported by Gholipour *et al.* (2020). The relatively high  $R^2$  of the estimated values is an indication of accuracy. Therefore, the PKOB produced at 318.15 K fitted well with the pseudo-second-order kinetic model.

The activation energies of PKOB using Itu/H<sub>2</sub>SO<sub>4</sub> catalyst for pseudo-first and pseudo-second order kinetic models were determined from Figures 7 and 8 and depicted in Table 8. It could be observed that the activation energy obtained from the pseudo-first-order model was lower than that of the second-order model. This shows that the production of biodiesel from PKO using the Itu/H<sub>2</sub>SO<sub>4</sub> catalyst requires lesser energy consumption in the first order model, which makes the process economical (Onukwuli *et al.*, 2018) than the second order model with an activation energy value of 46,259.1 KJ/mol.

### **Kinetics of Palm Kernel Oil Biodiesel Reactions**

The kinetic study was done on the stage between 60 to 180 min that the rate of reaction was considerable, with an optimum catalyst concentration (1 wt%, Itu/H<sub>2</sub>SO<sub>4</sub>) at 318.15 to 338.15 K. Pseudo first and second order reaction kinetics was assumed for the transesterification reaction of palm kernel oil biodiesel (PKOB) from Equation 13 and 16 respectively. To establish the correctness of these assumptions and estimate the values of the reaction constants  $k$  at various temperatures, plots of  $\ln(1-X_{EE})$  versus time (min) and  $1/(1-X_{EE})$  versus time at temperatures 318.15, 328.15 and 338.15 K were made for the pseudo first and second order reaction, respectively. The plots generated using values presented in Tables 5 to 7 are presented in Figures 1 to 6, while values of correlation coefficients  $R^2$  and rate constants that were determined from the slope of the trend line are presented in Table 4. The values of correlation coefficients ( $R^2$ ) of the pseudo first and second order reaction at 318.15 K and 328.15 K were higher than those obtained at 338.15 K, with the  $R^2$  value recorded for second order kinetics at 318.15 K having the highest value of 0.983. This is similar to the results reported by Gholipour *et al.* (2020). The relatively high  $R^2$  of the estimated values is an indication of accuracy. Therefore, the PKOB produced at 318.15 K fitted well with the pseudo-second-order kinetic model.

The activation energies of PKOB using Itu/H<sub>2</sub>SO<sub>4</sub> catalyst for pseudo-first and pseudo-second order kinetic models were determined from Figures 7 and 8 and depicted in Table 8. It could be observed that the activation energy obtained from the pseudo-first-order model was lower than that of the second-order model. This shows that the production of biodiesel from PKO using the Itu/H<sub>2</sub>SO<sub>4</sub> catalyst requires lesser energy consumption in the

first order model, which makes the process economical (Onukwuli *et al.*, 2018) than the second order model with an activation energy value of 46,259.1 KJ/mol.

**Table 4: Kinetic Data of PKOB using Itu/H<sub>2</sub>SO<sub>4</sub> Catalyst**

Temperature (K)	1 <sup>st</sup> Order, K <sub>1</sub> (min <sup>-1</sup> )	R <sup>2</sup>	2 <sup>nd</sup> Order, K <sub>2</sub> (ml/mol.min <sup>-1</sup> )	R <sup>2</sup>
318.15	0.0003	0.97	0.032	0.98
328.15	0.0006	0.92	0.096	0.88
338.15	0.0004	0.48	0.069	0.35

**Table 5: Values used to plot PKOB Kinetics at 318.15 K**

Time (minutes)	X <sub>EE</sub>	1-X <sub>EE</sub>	-ln(1-X <sub>EE</sub> )	1/(1-X <sub>EE</sub> )
1.00	0.876	0.124	2.087	8.065
2.00	0.904	0.096	2.343	10.417
3.00	0.916	0.084	2.477	11.905

**Table 6: Values used to plot PKOB Kinetics at 328.15 K**

Time (minutes)	X <sub>EE</sub>	1-X <sub>EE</sub>	-ln(1-X <sub>EE</sub> )	1/(1-X <sub>EE</sub> )
60.00	0.892	0.108	2.226	9.259
120.00	0.912	0.088	2.430	11.364
180.00	0.952	0.048	3.037	20.833

**Table 7: Values used to plot PKOB Kinetics at 338.15 K**

Time (minutes)	X <sub>EE</sub>	1-X <sub>EE</sub>	-ln(1-X <sub>EE</sub> )	1/(1-X <sub>EE</sub> )
60.00	0.948	0.052	2.957	19.231
120.00	0.960	0.04	3.219	25.000
180.00	0.908	0.092	2.386	10.870

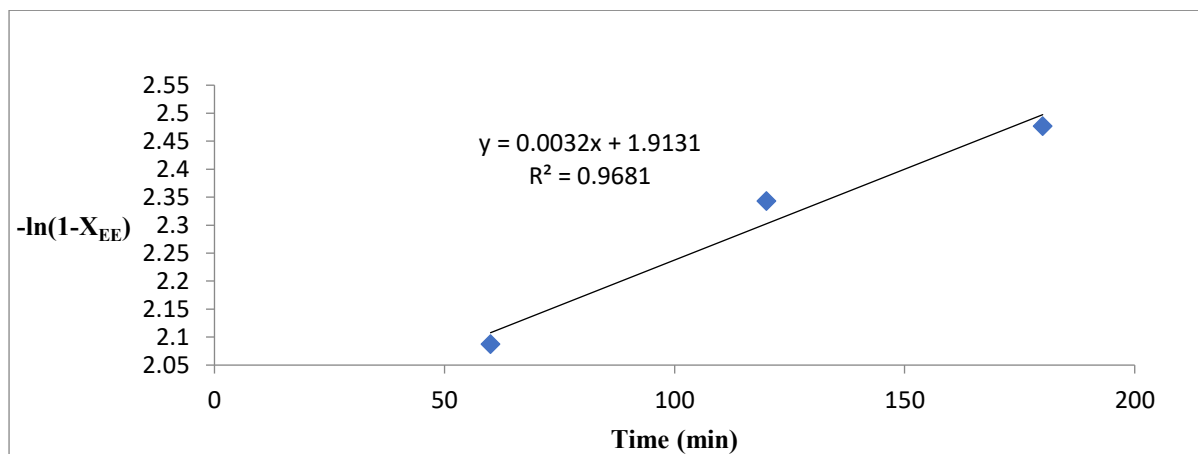


**Figure 1: Pseudo-first Order Kinetics at 318.15 K**

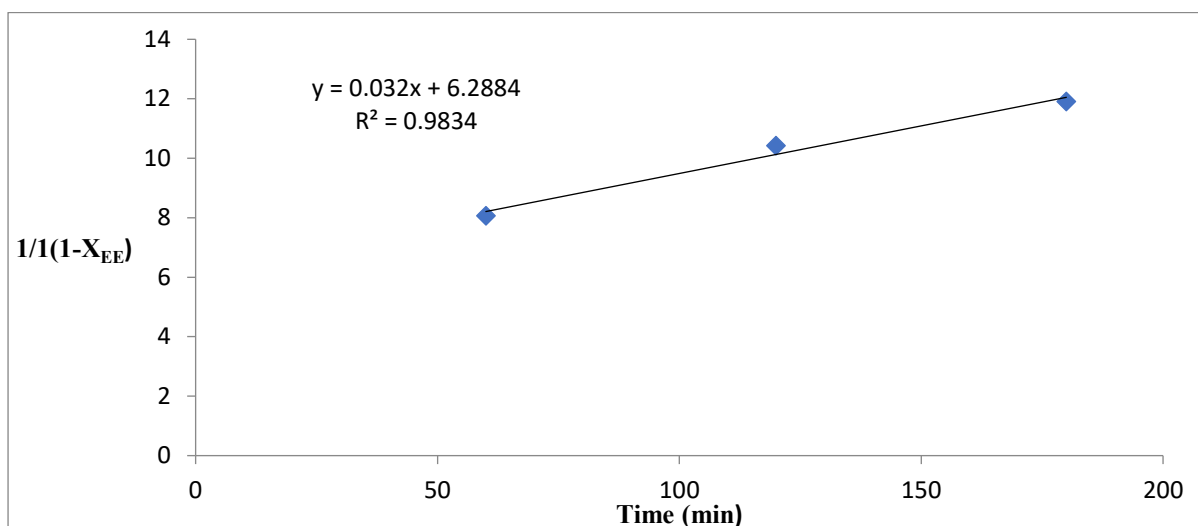


Figure 2: Pseudo-second Order Kinetics at 318.15 K

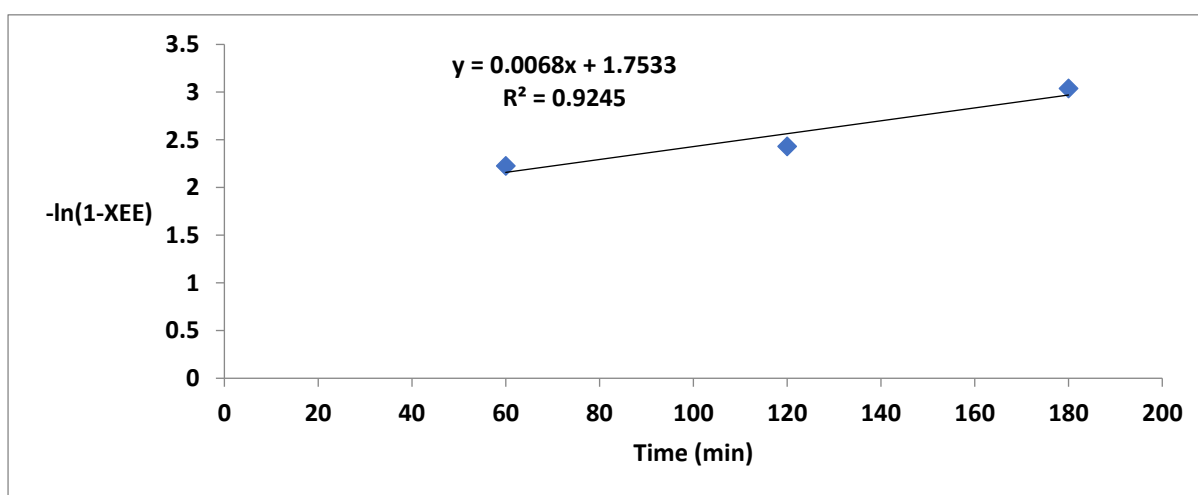


Figure 3: Pseudo-first order kinetics at 328.15 K

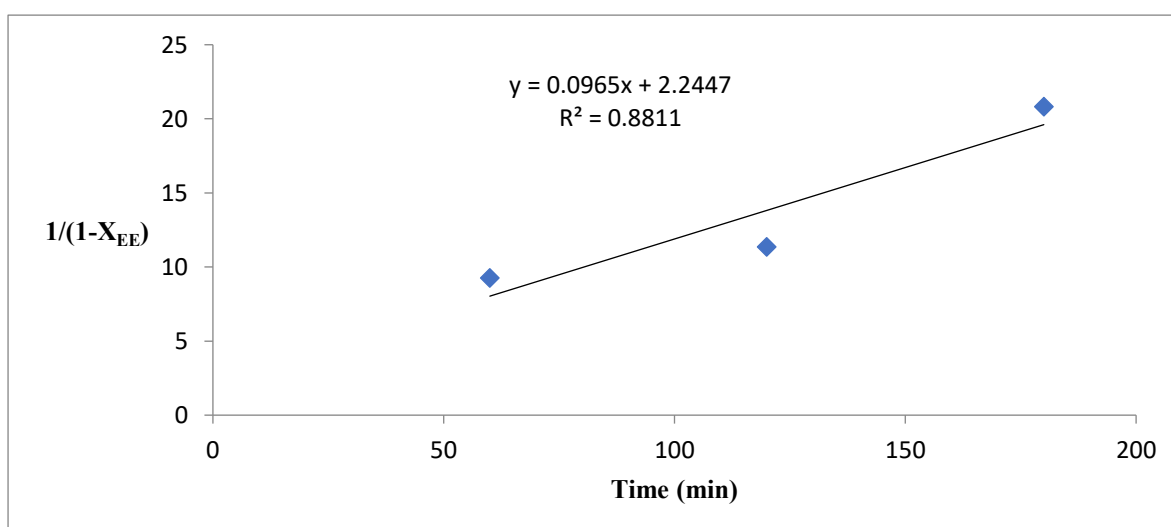


Figure 4: Pseudo-second order kinetics at 328.15 K



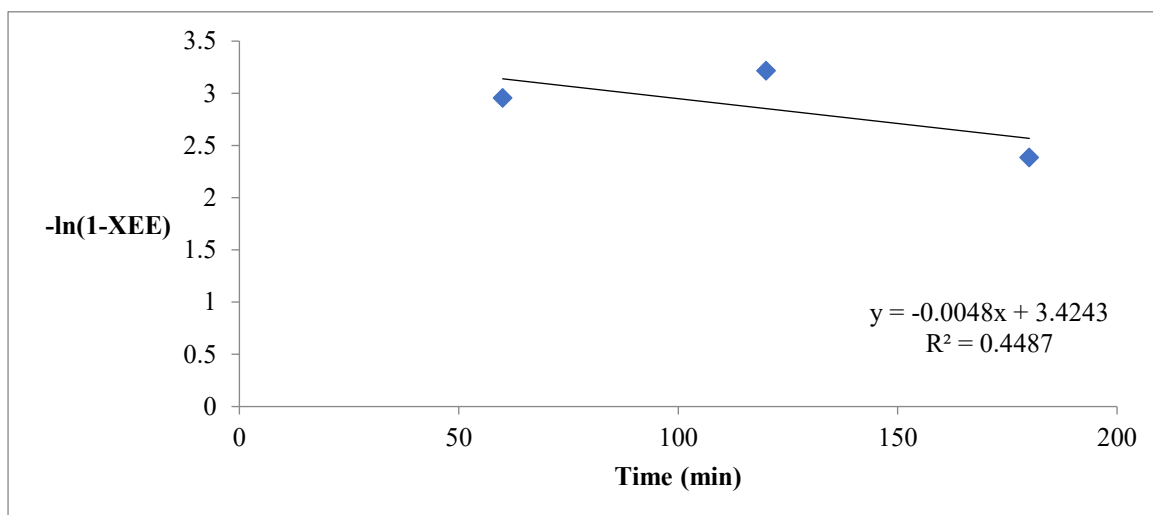


Figure 5: Pseudo-first order kinetics at 338.15 K

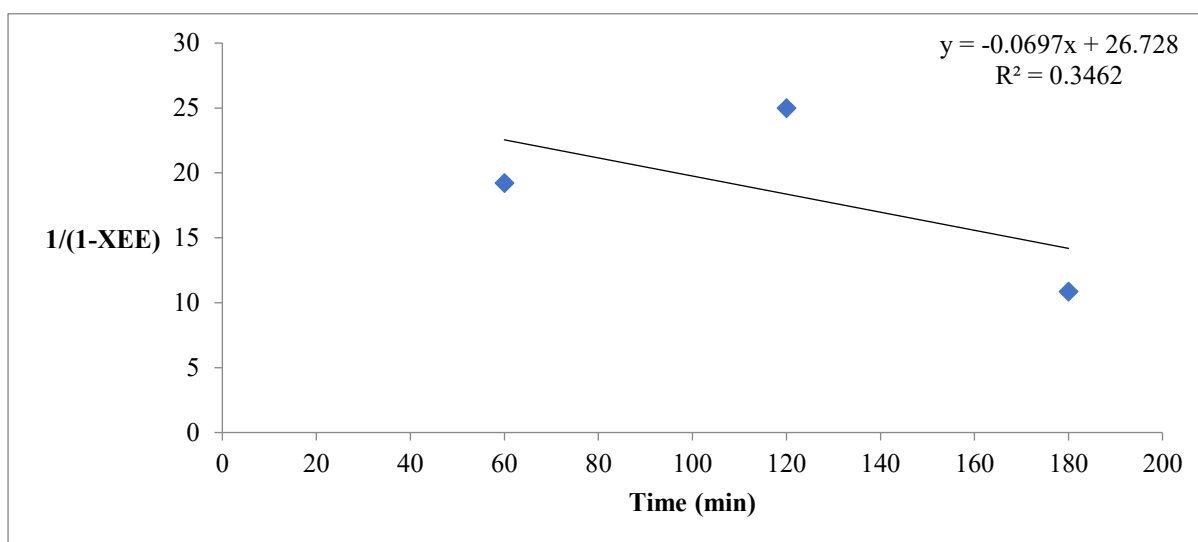


Figure 6: Pseudo-second order kinetics at 338.15 K

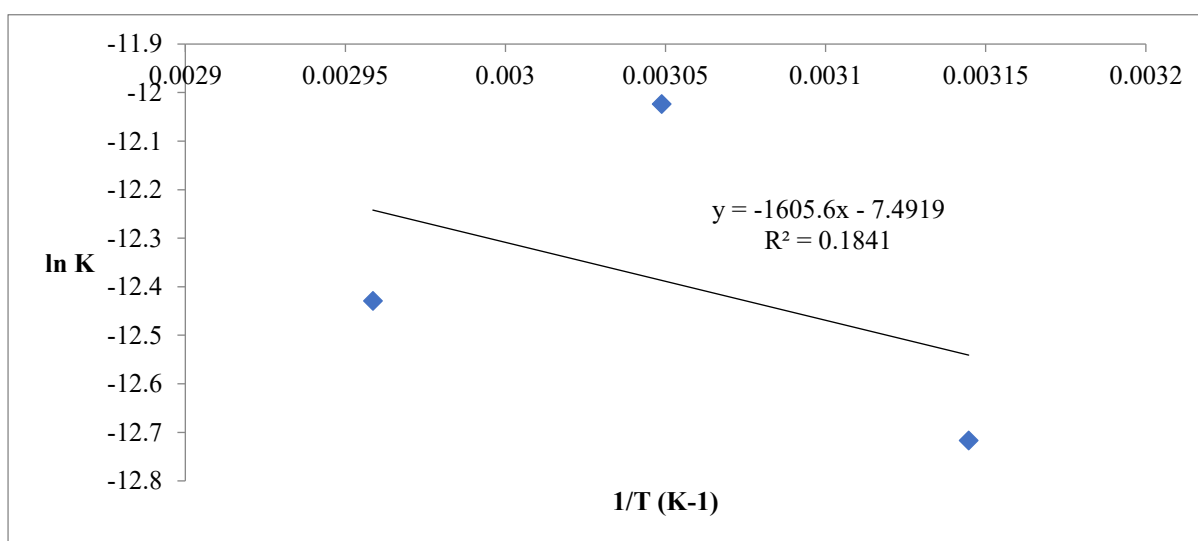


Figure 7: Determination of Activation energy ( $E_a$ ) for pseudo-first order reaction

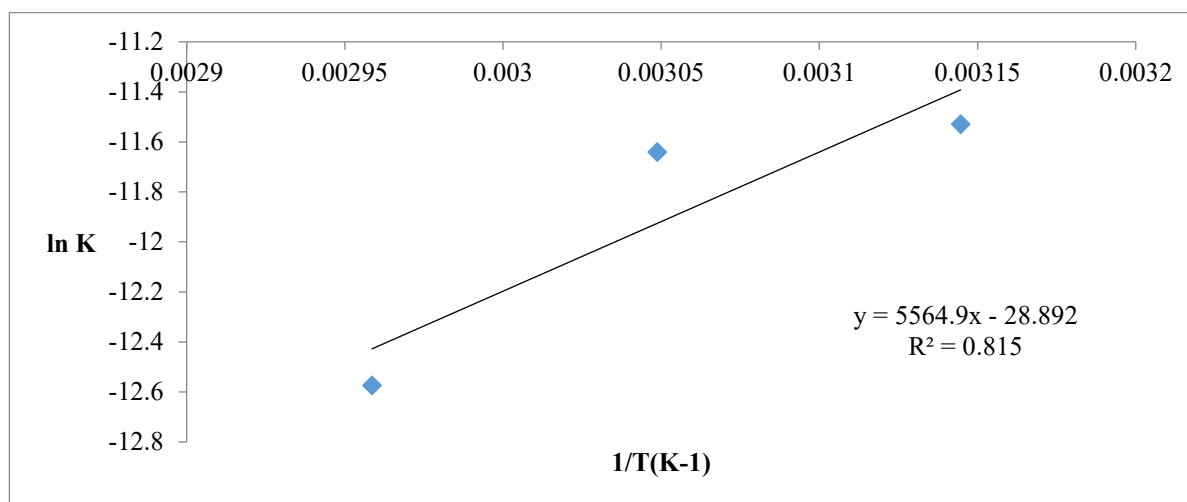


Figure 8: Determination of activation energy ( $E_a$ ) for pseudo-second order reaction

Table 7: Activation Energies ( $E_a$ ) of PKOB using Itu/ $H_2SO_4$  Catalyst

1 <sup>st</sup> Order				
Temperature (K)	1/T (K <sup>-1</sup> )	K <sub>1</sub> (min <sup>-1</sup> )	Ln K	Activation energy (E <sub>a</sub> )
318.15	0.00314	0.000003	-12.717	13,343.9 kJ/mol
328.15	0.00305	0.000006	-12.024	
338.15	0.00296	0.000004	-12.429	
2 <sup>nd</sup> Order				
318.15	0.00314	0.0000098	-11.530	46,259.1 kJ/mol
328.15	0.00305	0.0000088	-11.640	
338.15	0.00296	0.0000035	-12.574	

## CONCLUSION

In the present study, the kinetic studies of the transesterification of palm kernel oil biodiesel and the effect of catalyst dosage on biodiesel yield were studied. The following deductions were drawn after the research:

The highest yield (96%) was achieved at a molar ratio (alcohol: oil) 12 to 1, a catalyst amount of 1 wt%, reaction temperature of 338.15 K, and stirring rate of 600 rpm in 2 h. The rate constant for the pseudo-first and second order reactions increased as temperature increased from 318.15 to 328.15 K. This indicates that the rate of the transesterification of PKO was favoured at higher temperatures and heat is required for the reaction. The activation energy determined for PKOB transesterification indicates that the pseudo-second order reaction requires more energy than pseudo-first order. This could be because of the presence of unsaturated fatty acid in the PKO.

## REFERENCES

Faisal, A., Javed, F., Hassan, M., Gorji, M., Akram, S., Rashid, N., and Rehman, F. (2021). Experimental and mathematical nonlinear rheological characterization of chicken fat oil, a sustainable feedstock for biodiesel. *Biomass Conversion and Biorefinery*, 1–8.

- Feyzi M., Hosseini N., Yaghobi N., and Ezzati R. (2017). Preparation, characterization, kinetic and thermodynamic studies of MgO-La<sub>2</sub>O<sub>3</sub> nanocatalysts for biodiesel production from sunflower oil. *Chemical Physics Letters*, **677**, 19-29.
- Gholipour, N. Z., Kamran, A. P., and Yazdanian, E. (2020). Biodiesel production in the presence of heterogeneous catalyst alumina: Study of kinetics and thermodynamics. *International Journal of Chemical Kinetics*, 1-13.
- Javed, F., Saif-ul-Allah, M. W., Ahmed, F., Rashid, N., Hussain, A., Zimmerman, W. B., and Rehman, F. (2022). Kinetics of biodiesel production from microalgae using microbubble interfacial technology. *Bioengineering*, **9** (12). 739.
- Li, X., Wang, Q., Wu, Y., Chen, J., Li, S., Ye, Y., Wang, D., and Zheng, Z. (2022). Optimization of key parameters using RSM for improving the production of the green biodiesel from FAME by hydrotreatment over Pt/SAPO-11. *Biomass and Bioenergy*, **158**, 106379
- Meher, L.C., Sagar, D.V., and Naik, S. (2006). Technical aspects of biodiesel production by transesterification—A review. *Renewable and Sustainable Energy Reviews*, **10**, 248–268.
- Pinzi, S., Gandia, L. M., Arzamendi, G., Ruiz, J. J., and Dorado, M, P. (2011). Influence of vegetable oils' fatty acid composition on reaction temperature and glycerides conversion to biodiesel during transesterification. *Bioresource Technology*, **102**, 1044-1050.
- Olutoye, M. A., and Hameed, B. H. (2016). Kinetics and deactivation of dual-site heterogeneous oxide catalyst during the transesterification of crude *jatropha* oil with methanol. *Journal of Taibah University for Science*, **10**(5), 685–699
- Onukwuli, O. D., and Callistus N. Ude, C. N. (2018). Kinetics of African pear seed oil (APO) methanolysis catalyzed by phosphoric acid-activated kaolin clay. *Applied Petrochemical Research*, **8**, 299–313.
- Yusuff, A. S., Adeniyi, O. D., Olutoye, M. A., and Akpan, U. G. (2018). Kinetic study of Transesterification of Waste Frying Oil to Biodiesel using Anthill-Eggshell-Ni-Co Mixed Oxide Composite Catalyst. *Petroleum and Coal*, **60**(1): 157-167.
- Zeinalipour-Yazdi C. D. (2018). On the possibility of an Eley–Rideal mechanism for Ammonia synthesis on Mn<sub>6</sub>N<sub>5+x</sub> (x = 1)-(111) surfaces. *Physical Chemistry Chemical Physics Journal*, **20**(27), 187,